

Article

Effect of Environmental Conditions on Strontium Adsorption by Red Soil Colloids in Southern China

Yang Shao ¹, Yuanyuan Zhao ^{1,2}, Min Luo ¹, Guifang Zhao ¹, Diandou Xu ¹, Zhiming Liu ² and Lingling Ma ^{1,*}

¹ Division of Nuclear Technology and Applications, Institute of High Energy Physics, Chinese Academy of Sciences, Beijing 100049, China

² State Key Laboratory of Chemical Resource Engineering, Beijing University of Chemical Technology, Beijing 100029, China

* Correspondence: malingling@ihep.ac.cn; Tel.: +86-10-88236403

Abstract: The fate of radionuclides in the environment is attracting increased attention. The effect of various environmental effects on the adsorption behavior of the strontium ion (Sr^{2+}) by red soil colloids in Southern China was studied by a series of batch experiments, and the adsorption mechanism was briefly investigated as well. With the increase in the solid–liquid ratio and the concentration of Sr^{2+} , the adsorption efficiency increased gradually. The effect of pH and ionic strength on adsorption was strong, while temperature had little effect. The adsorption data fitted to the Langmuir model indicates that the process is monolayered and homogeneous. The thermodynamic parameters also show that the adsorption of Sr^{2+} on red soil colloids is a spontaneous and exothermic process. The aim of this work is to gain insight into the role of red soil colloids on the fate of radionuclides in the field.

Keywords: strontium (Sr^{2+}); soil colloid; adsorption; China



Citation: Shao, Y.; Zhao, Y.; Luo, M.; Zhao, G.; Xu, D.; Liu, Z.; Ma, L. Effect of Environmental Conditions on Strontium Adsorption by Red Soil Colloids in Southern China. *Processes* **2023**, *11*, 379. <https://doi.org/10.3390/pr11020379>

Academic Editor: Carlos Sierra Fernández

Received: 29 December 2022

Revised: 16 January 2023

Accepted: 17 January 2023

Published: 25 January 2023



Copyright: © 2023 by the authors. Licensee MDPI, Basel, Switzerland. This article is an open access article distributed under the terms and conditions of the Creative Commons Attribution (CC BY) license (<https://creativecommons.org/licenses/by/4.0/>).

1. Introduction

Increased attention has been paid to the environmental behavior of radionuclides, especially since the Fukushima nuclear accident in 2011. In 2005, the activity value of ^{90}Sr in Fukushima Prefecture was $3.6 \text{ Bq}\cdot\text{kg}^{-1}$, while the activity value increased to hundreds or more $\text{Bq}\cdot\text{kg}^{-1}$ near Fukushima Daiichi nuclear power plant after the nuclear accident [1]. As a typical artificial radionuclide, ^{90}Sr with a half-life of 28.5 years, is produced by ^{235}U and ^{239}Pu nuclear fission, and is commonly released into the environment due to nuclear weapon tests, nuclear power plant accidents, and nuclear fuel reprocessing industries [2].

As one of the most toxic radionuclides, ^{90}Sr ion has a chemical behavior similar with calcium [3], which could potentially cause great external radiation doses and internal radiation to humans and other living things [4–6]. ^{90}Sr eventually enters the food chain by various ways from soil, under some conditions, and could further harm the health of plants, animals, and humans [7,8]. Therefore, it is crucial to study the behavior of Sr^{2+} in the soil since the stable Sr^{2+} presented a similar chemical migration with radionuclide $^{90}\text{Sr}^{2+}$.

Soil colloids, as the most active component in the soil with a size of 1 nm–1000 nm, perform a significant role in the migration of pollutants in the soil [9]. According to the composition, soil colloids are categorized into inorganic colloids, organic colloids, and organic-inorganic composite colloids. The behavior of Sr^{2+} adsorbed by inorganic colloids of Na-rectorite was studied using the static batch method. It was found that the adsorption process was affected by the pH value and ionic strength [10]. It was also reported that bentonite colloids had a significant retardation of the migration of Sr^{2+} with very slow flow rates of $1 \text{ mL}\cdot\text{h}^{-1}$ [11]. For the organic colloids, most studies focused on the effects of the reprehensive organic matter of humic acids (HA), and it was found that HA had different effects on the migration of radionuclides under different conditions [12–14]. The effect of HA on the adsorption of ^{137}Cs , ^{133}Ba , and ^{154}Eu was studied [15]. It was found that adding HA has no obvious effect on the adsorption of Cs^+ at pH 3–10. For Ba^{2+} , HA

promoted the adsorption when the pH value was lower than 6.4. However, HA inhibited the adsorption when the pH was higher than 6.4. Furthermore, HA had a significant impact on the adsorption of Eu^{3+} . Therefore, it can tell that HA had different effects on different nuclides. In fact, the organic-inorganic composite colloid is the most ubiquitous colloid in nature. However, more attention has been paid on the artificially synthetic composite colloids in the lab [16]. There are relatively few reports on red colloids as organic-inorganic colloids extracted from arable soils. The current studies on the adsorption of Sr^{2+} were mainly focused on the artificial inorganic colloids, the synthetic composite colloids or natural whole soil without considering the effect of size [17]. The behavior of U^{6+} on the red soil colloid was studied by a static method, the effects of various factors on adsorption processes have been discussed, and the significant role of organic matters in the migration of U^{6+} in soil has been confirmed [18]. Red soil is the most extensively distributed soil in Southern China [19]. However, there is no study about the adsorption of strontium in red soil colloids in China [20]. To further assess the effect of strontium on the ecosystem, it is necessary to study real soil colloids on the fate of Sr^{2+} in the field.

In the present study, the adsorption behavior of Sr^{2+} on soil colloids extracted from red soil is investigated to check the effect of environmental effects on Sr^{2+} adsorption by a series of batch experiments. The sorption mechanism between colloids and Sr^{2+} is explored, which is of some significance for the future study of the migration behavior of radionuclides in soil.

2. Materials and Methods

2.1. Materials

Materials: Strontium nitrate, nitric acid, sodium hydroxide, and hydrogen peroxide (Analytical grade, Beijing chemical plant). Deionized water ($>18.2 \text{ M}\Omega \text{ cm}^{-1}$) was obtained from the Milli-Q system, and anhydrous ethanol were obtained from commercial sources.

2.2. Sampling and Colloid Extraction

The arable surface red soil was collected in Hunan Province ($28^{\circ}19' \text{ N}$, $112^{\circ}98' \text{ E}$), which is a typical red soil area in southern China. The study area is a subtropical monsoon climate with abundant rainfall. Soil colloids were prepared by the method of sedimentation siphoning performed in accordance with Stokes law [21]. In our study, we selected the stable Sr element to simulate the behavior of radioactive Sr. There were two Sr compounds that could be used in our study, which were $\text{Sr}(\text{NO}_3)_2$ and SrCO_3 . However, the solubility of $\text{Sr}(\text{NO}_3)_2$ is better than SrCO_3 . Therefore, $\text{Sr}(\text{NO}_3)_2$ was selected for the adsorption study. Deionized water was used in the experiments.

2.3. Inorganic Colloid

The effect of organic matter on the adsorption of Sr^{2+} from soil colloids was studied by using H_2O_2 to remove the organic matter in the soil colloids [21,22]. A certain amount of H_2O_2 was added into the soil colloids, and the soil was put in a heated water bath to evaporate until no bubbles were present. Finally, the supernatant was discarded by means of centrifugation. The matter at the bottom of centrifuge tube was the inorganic soil colloids.

2.4. Batch Adsorption Experiments

All experiments were conducted using a batch method on a thermostated oscillator. A centrifuge tube with 4 mg of soil colloids and $100 \text{ mg}\cdot\text{L}^{-1}$ of $\text{Sr}(\text{NO}_3)_2$ was placed in the water bath thermostated oscillator with a contact time of 12 h at room temperature (25°C). Then, the solution was filtered through a $0.1 \mu\text{m}$ filter.

The adsorption efficiency and the adsorption capacity (Q_e , mg g^{-1}) was calculated by Equations (1) and (2). The data were measured by ICP-MS (Inductively coupled plasma mass spectrometry, Thermo-X7, Thermo Scientific, Waltham, MA, USA).

$$\text{Adsorption efficiency} = \frac{C_0 - C_t}{C_0} \times 100 \% \quad (1)$$

$$Q_e = \frac{C_0 - C_t}{m} \times V \quad (2)$$

where C_0 is the concentration of Sr^{2+} solution before adsorption ($\text{mg}\cdot\text{L}^{-1}$), and C_t is the concentration of Sr^{2+} at a certain time after adsorption ($\text{mg}\cdot\text{L}^{-1}$). m and V are the weight (g) of soil colloid, and the volume (L) of the solution used in the adsorption experiment [23].

The effects of these factors on the adsorption were studied by changing the amount of soil colloids and varying the strontium nitrate concentration, ionic strength, temperature, pH values, and organic carbon.

2.5. Characterization

The particle size was measured by a Nano particle size analyzer (Zetasizer Nano ZS90, Malvern, England). The contents of the major elements in the soil colloids were analyzed by X-ray Fluorescence (XRF, Eagle III XXL μ -Probe, EDAX Inc., Pleasanton, CA, USA). The content of the soil's total C, N, and S was measured using an organic elemental analyzer (Vario EL Cube, Elementar, Germany).

3. Results and Discussion

3.1. The Properties of Soil Colloid

In the colloidal extraction process, we took the last extract and diluted it 10–20 times to characterize the particle size. Table 1 shows the analytical results of the basic properties of the soil colloids.

Table 1. Basic properties of the red soil colloids (%).

Soil	TN	TS	TC	SiO_2	Al_2O_3	Fe_2O_3	CaO
%	0.30	0.03	2.87	53.15	30.92	11.95	0.49

Remarks: TN represents the total nitrogen in soil colloids; TS represents the total sulfur in soil colloids; TC represents the total carbon in soil colloids.

3.2. Colloid Dosage

The initial concentration of Sr^{2+} was $100 \text{ mg}\cdot\text{L}^{-1}$, and the amount of soil colloids were 2, 4, 6, 8, and 10 mg, respectively; these quantities were used to calculate the adsorption efficiency. As is shown in Figure 1, with the increase in the solid-to-liquid ratio, the adsorption capacity gradually increased. In the first five minutes of the reaction, the adsorption efficiency increased rapidly, the maximum adsorption efficiency increased from 0% to 13%, which may be attributed to more available adsorption sites at the beginning of the reaction. After half an hour, the adsorption reaction basically was kept in an equilibrium.

When the colloid dosage was increased from 2 mg to 10 mg, the adsorption efficiency increased from 2% to 13% with the adsorption capacity of 8.42, 7.51, and $6.41 \text{ mg}\cdot\text{g}^{-1}$, respectively. An increase in the amount of colloids provided more adsorption on the active sites or participation of the number of adsorption functional groups, and enhanced the colloidal surface adsorption capacity. The adsorption rate was faster when the concentration changed from 2 mg to 4 mg, resulting in the steep rise of adsorption efficiency. Additionally, more soil colloids would result in the adsorption capacity when the same Sr concentration was used. Since the concentration of Sr was stable, the adsorption capacity decreased when the adsorption efficiency increased, which is consistent with a similar previous study of U(VI) [24].

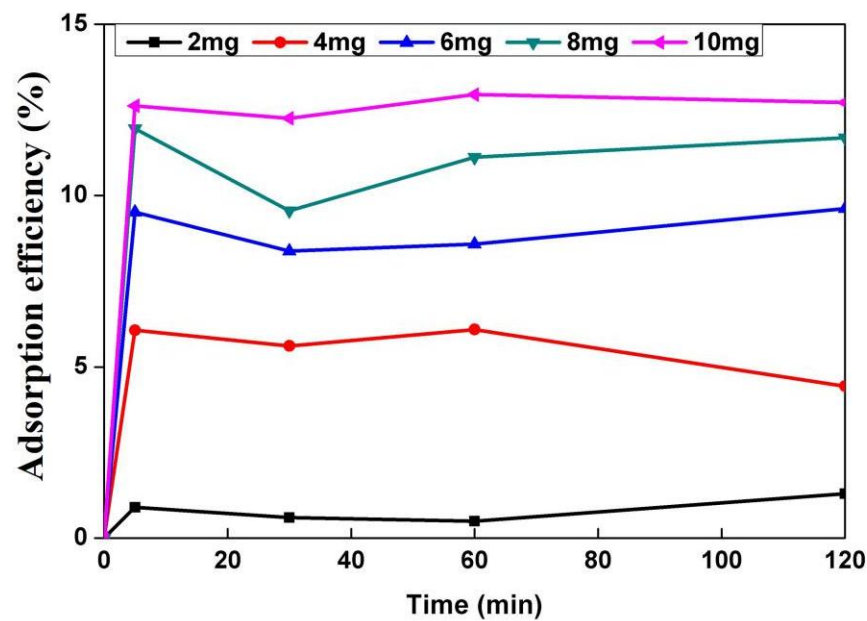


Figure 1. Effect of soil colloid dosage on the sorption of Sr on soil colloids. $T = 25 \pm 1 \text{ }^\circ\text{C}$, $C[\text{Sr}^{2+}]_{\text{initial}} = 100 \text{ mg}\cdot\text{L}^{-1}$, $\text{pH} = 7 \pm 0.1$.

3.3. Effect of pH

As shown in Figure 2, the adsorption efficiency was approximately 2% at $\text{pH} = 5$, and it increased to 7% with an increase in the pH to 7. At a pH of 3–10, Sr was present in the form of Sr^{2+} ; therefore, the adsorption behavior was dependent on the negative charge on the soil colloid surface [25]. With the increase of the pH value, the dissociation of negative minerals on the clay minerals, organic matter, and oxide surface in the soil colloid was promoted, thereby increasing the number of negative charges on the colloidal surface [26]. Therefore, the subsequent experimental $\text{pH} = 6$ value was selected.

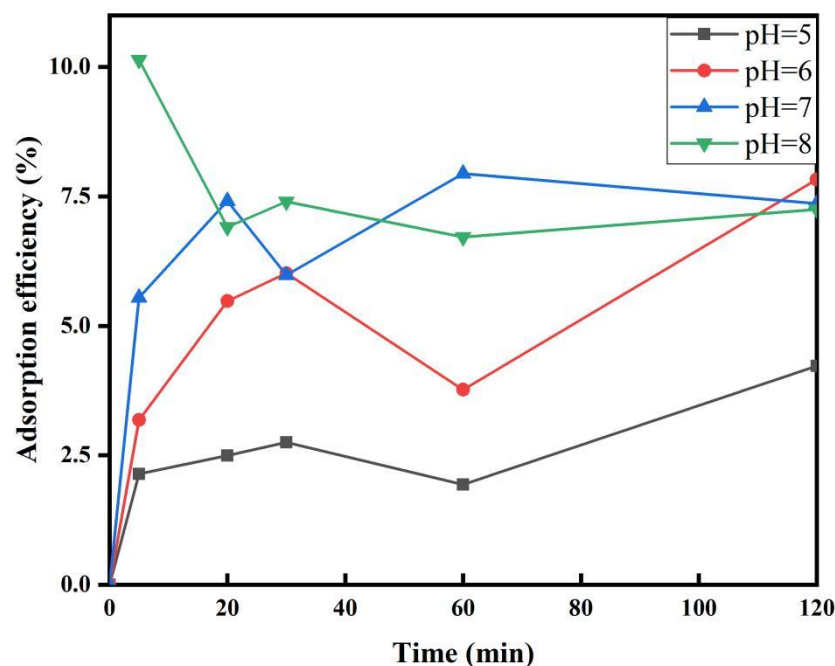


Figure 2. Effect of pH on the sorption of Sr on soil colloids. $T = 25 \pm 1 \text{ }^\circ\text{C}$, $C[\text{Sr}^{2+}]_{\text{initial}} = 100 \text{ mg}\cdot\text{L}^{-1}$, soil-liquid rate = $800 \text{ mg}\cdot\text{L}^{-1}$.

3.4. Effect of Ionic Strength

The effect of ionic strength on the sorption process is shown in Figure 3. It was clearly found that the ionic strength has a significant inhibiting effect on the adsorption. As the ionic strength increased from $0.001 \text{ mol}\cdot\text{L}^{-1}$ to $0.1 \text{ mol}\cdot\text{L}^{-1}$, the adsorption efficiency decreased from 10% to 3%. One reason for this may be that the ionic strength affected the electrostatic interaction of the colloidal surface. A high ionic strength would weaken the repulsive force, causing agglomeration, which decreases the number of available adsorption sites. On the other hand, the presence of electrolytes on the adsorption, mainly due to the cationic ions and Sr^{2+} produce competitive adsorption sites for the adsorption on the colloidal surface [27,28]. The results obtained were similar to the sorption of Sr^{2+} on a magnetic adsorbent and on montmorillonite [29,30]. It was also reported that the adsorptions of the Sr^{2+} and U^{6+} on the Na-rectorite decreased with an increase in ionic strength [27].

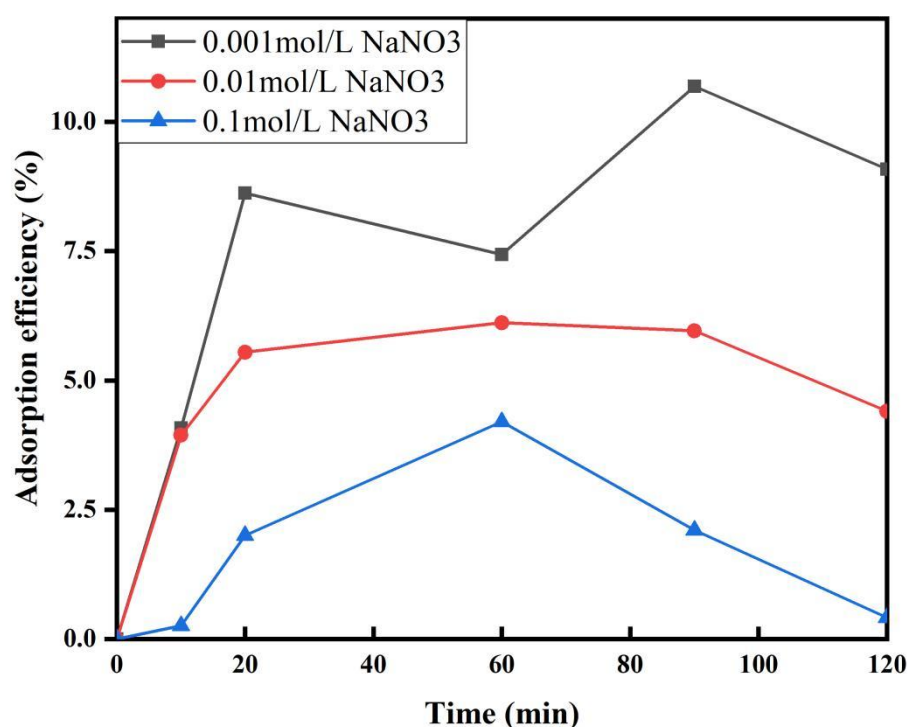


Figure 3. Effect of different ionic strength on the sorption of Sr on soil colloids. $T = 25 \pm 1 \text{ }^\circ\text{C}$, $[\text{Sr}^{2+}]_{\text{initial}} = 100 \text{ mg}\cdot\text{L}^{-1}$, soil-liquid rate = $0.8 \text{ g}\cdot\text{L}^{-1}$, $\text{pH} = 6 \pm 0.1$.

3.5. Effect of Initial Sr^{2+} Concentration

As shown in Figure 4, the adsorption efficiency increased from 2% to 17% with the increase in the initial concentration of Sr^{2+} . When the interaction between the colloids and the strontium equilibrated, the adsorption efficiency slowed down, and as the initial concentration increased, the residual unreacted strontium ion concentration increased, and the adsorption efficiency decreased.

To explore the adsorption mechanism of Sr^{2+} by colloids, the adsorption data was fitted with Langmuir and Freundlich adsorption isotherm models [31,32]. The soil colloid adsorption of different concentrations of strontium nitrate was the data used for the isothermal fitting [33]. The modeled results are provided in Table 2. The correlation coefficient (R^2) calculated by Langmuir model was higher, which suggests that the Langmuir isotherm model is more suitable to describe the adsorption process and the sorption sites on the colloids are homogeneously distributed. The major sorption mechanism is monolayer sorption. The modeling adsorption capacity Q_{max} was $11.27 \text{ mg}\cdot\text{g}^{-1}$, which was similar with the real soil colloids of $11.50 \text{ mg}\cdot\text{g}^{-1}$.

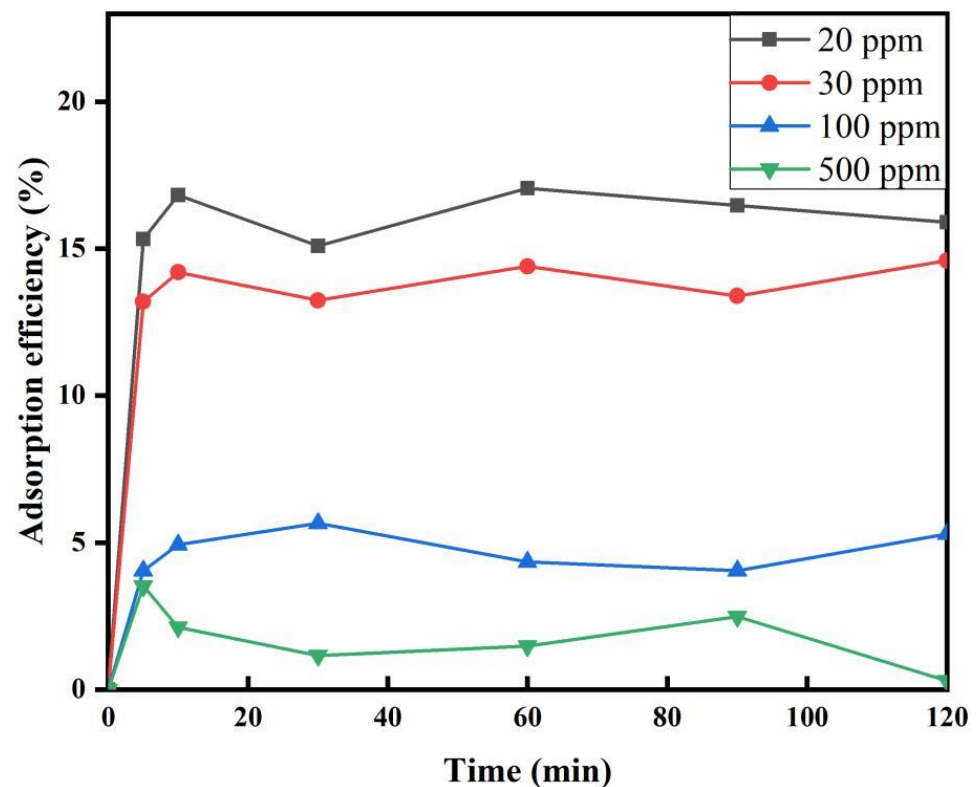


Figure 4. Effect of strontium nitrate concentration on the sorption of Sr on soil colloids. $T = 25 \pm 1$ °C, soil-liquid rate = $800 \text{ mg}\cdot\text{L}^{-1}$, $\text{pH} = 6 \pm 0.1$.

Table 2. Parameters for the Langmuir and Freundlich isotherm models at different initial concentrations.

Langmuir			Freundlich		
Q_m ($\text{mg}\cdot\text{g}^{-1}$)	b ($\text{L}\cdot\text{mol}^{-1}$)	R^2	K_F ($\text{mol}^{1-n}\cdot\text{L}^n\cdot\text{g}^{-1}$)	n	R^2
11.27	29.40	0.9346	1.32	3.30	0.9062

3.6. Effect of Organic Matter

As shown in Figure 5A, the adsorption efficiency was significantly decreased by 40% after removal of soil organic matter. The adsorption efficiency increased with the increase in the concentration of HA. As shown in Figure 5B, the concentration of HA from 0 to $100 \text{ mg}\cdot\text{L}^{-1}$, the adsorption efficiency increased by approximately 36%. These may be attributed to the polar groups in the soil organic matter (such as hydroxyl, carboxyl, etc.), which enhanced the adsorption of Sr^{2+} by providing a large number of negative charges as important complexing agents [34,35].

This study confirms the important role that organic matter performs in the adsorption of Sr^{2+} by real soil colloids, which were proposed by previous studies on synthesized colloids [10,36].

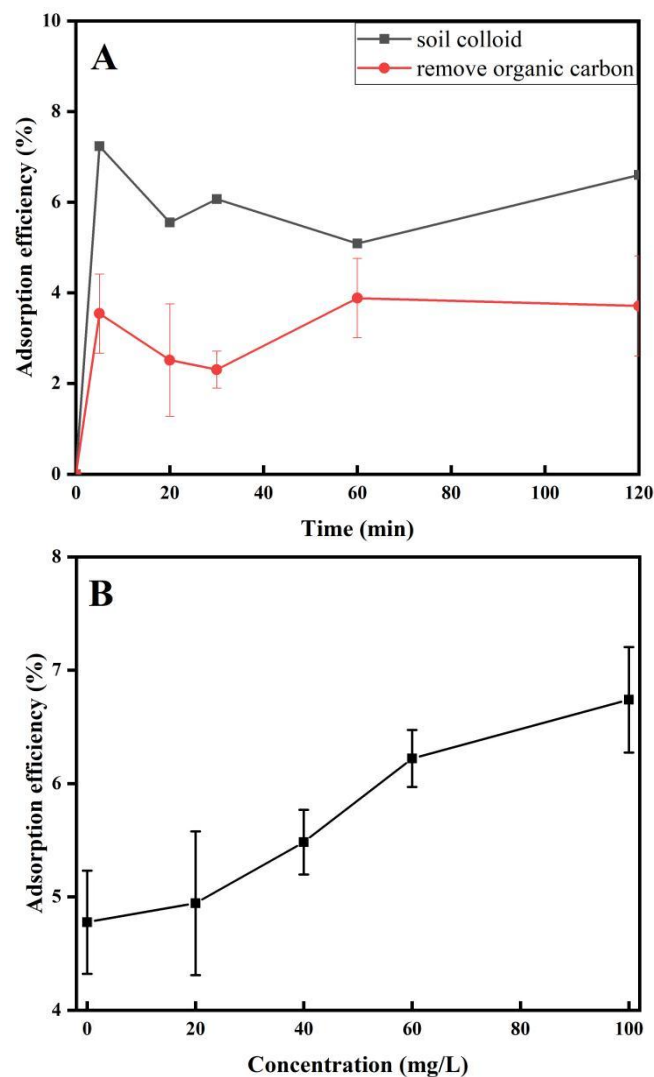


Figure 5. Effect of organic matter (A) and Effect of different concentration of HA (B) on the sorption of Sr on soil colloids. $T = 25 \pm 1 \text{ }^\circ\text{C}$, soil-liquid rate = $0.8 \text{ g}\cdot\text{L}^{-1}$, $\text{pH} = 6 \pm 0.1$, $C[\text{Sr}^{2+}]_{\text{initial}} = 100 \text{ mg}\cdot\text{L}^{-1}$.

3.7. Sorption Kinetic

To examine the controlling mechanism of the adsorption process, the pseudo-first order kinetic and pseudo-second order kinetic models were employed to examine the experimental data at an initial concentration of $100 \text{ mg}\cdot\text{L}^{-1}$ at pH 6, $25 \text{ }^\circ\text{C}$, and the soil-liquid rate of $0.80 \text{ g}\cdot\text{L}^{-1}$ according to Equations (2) and (3) [37,38]:

$$Q_t = Q_e \cdot (1 - \exp(-K_1 t)) \quad (3)$$

$$\frac{t}{Q_t} = \frac{1}{K_2 Q_e^2} + \frac{1}{Q_e} t \quad (4)$$

where Q_t ($\text{mg}\cdot\text{g}^{-1}$) and Q_e ($\text{mg}\cdot\text{g}^{-1}$) represents the amount of Sr^{2+} adsorbed at a moment and at equilibrium time, t (min) is the shaking time, and K_1 (min^{-1}) and K_2 ($\text{g}\cdot\text{min}^{-1}\cdot\text{mg}^{-1}$) are pseudo-first order kinetic and pseudo-second order kinetic adsorption parameters, respectively.

The kinetic results and parameters are shown in Figure 6 and Table 3. It was found that a better fit was obtained for the pseudo-second order model ($R^2 = 0.9918$) compared with the pseudo-first order model ($R^2 = 0.9579$), which indicates that Sr^{2+} was chemically adsorbed by the colloids. The value of Q_m was $5.63 \text{ mg}\cdot\text{g}^{-1}$, which was much higher than the red soil colloids analyzed in this study ($2.90 \text{ mg}\cdot\text{g}^{-1}$).

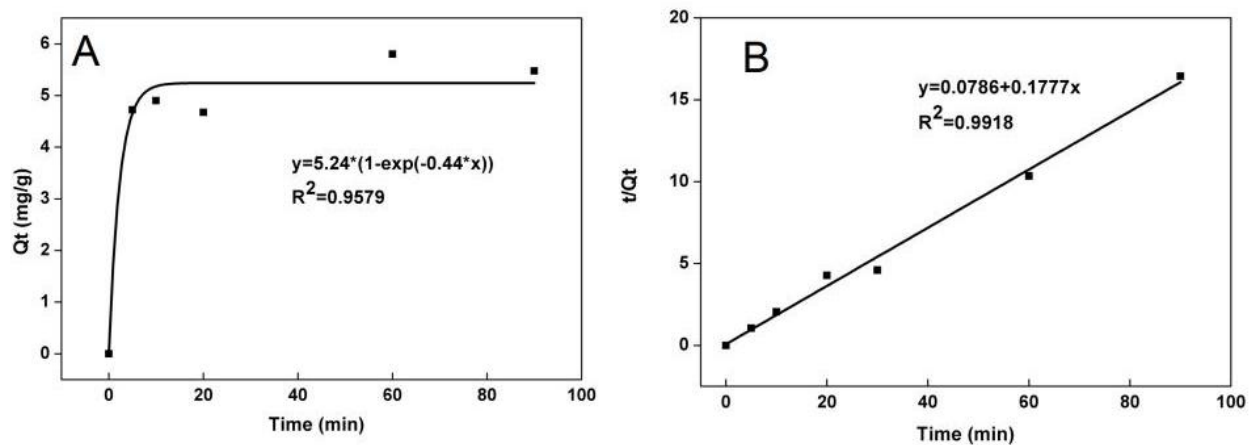


Figure 6. Fitting results of first-order kinetic and second-order kinetic. (A) for first-order kinetic and (B) for second-order kinetic.

Table 3. Values of kinetics parameters for the adsorption of Sr on soil colloid.

First-Order Kinetic			Second-Order Kinetic		
Q_m ($\text{mg}\cdot\text{g}^{-1}$)	K_1 (min^{-1})	R^2	Q_m ($\text{mg}\cdot\text{g}^{-1}$)	K_2 ($\text{g}\cdot\text{min}^{-1}\cdot\text{mg}^{-1}$)	R^2
5.24	0.58	0.9579	5.63	0.40	0.9918

3.8. Adsorption Thermodynamics

As shown in Figure 7, the adsorption quantity gradually increased with the increasing of temperature. The data were fit to the thermodynamic model. Thermodynamic parameters are listed in Table 4, include the Gibbs energy (ΔG), enthalpy (ΔH), and entropy (ΔS) were calculated from the following equations [39,40]:

$$\ln K_D = -\frac{\Delta H^0}{RT} + \frac{\Delta S^0}{R} \quad (5)$$

$$\Delta G = \Delta H - T\Delta S^0 \quad (6)$$

where K_D is solid–liquid partition coefficient; Q_e is adsorption equilibrium when adsorption; C_e is concentration of adsorption equilibrium; R ($8.314 \text{ J}(\text{mol}\cdot\text{K})^{-1}$) is the ideal gas constant; and T is the Kelvin temperature.

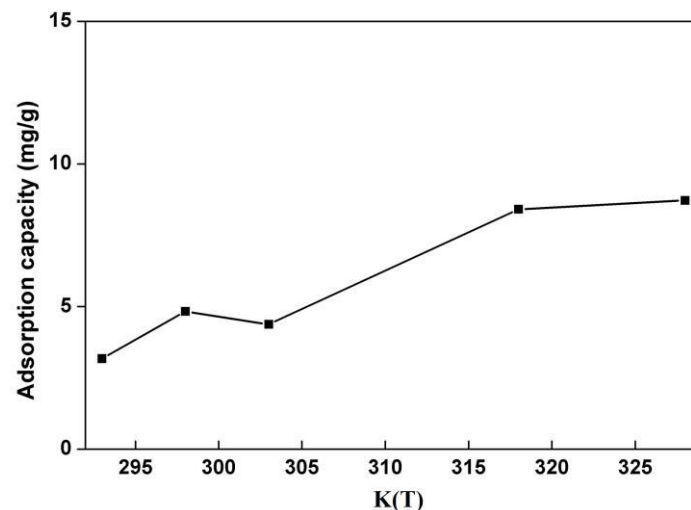


Figure 7. Effect of temperature on adsorption of Sr on soil colloids. Soil-liquid rate = $0.8 \text{ g}\cdot\text{L}^{-1}$, $\text{pH} = 6 \pm 0.1$, $C[\text{Sr}^{2+}]_{\text{initial}} = 100 \text{ mg}\cdot\text{L}^{-1}$.

Table 4. Values of thermodynamic parameters for the adsorption of Sr on soil colloid, T = 293/298/303/318/328 K, soil-liquid rate = 0.8 g·L⁻¹, pH = 6 ± 0.1, strontium nitrate concentration = 100 mg·L⁻¹.

Temperature (K)	ΔG (KJ·mol ⁻¹)	ΔS^0 (KJ·(mol·K) ⁻¹)	ΔH^0 (KJ·mol ⁻¹)
293	−8.96		
298	−9.53		
303	−10.09	0.1130	24
318	−11.78		
328	−12.90		

The positive ΔH indicates that the adsorption of Sr²⁺ by soil colloids is an endothermic process in the environment. With the increase in temperature, the adsorption efficiency increased, which is consistent with the above reported results. In addition, when ΔH was less than 30 KJ·mol⁻¹, it meant that most of the adsorption reactions under this condition are physical adsorption. The positive ΔS and negative ΔG suggests that the adsorption process is a spontaneous and entropy increased reaction at the solid/solution colloid interface during the adsorption. It was found in the adsorption behavior of Sr on bentonite that the negative ΔH and ΔG indicated that the adsorption progress was exothermic and spontaneous [41].

4. Conclusions

The adsorption of a typical radionuclide of Sr²⁺ by composite colloids extracted from red soil in China was investigated for the first time. It was found that the soil organic matter played an important role in the process and the pH. The adsorption process in nature was in accordance with second order kinetics and the Langmuir adsorption isotherm, and spontaneously proceeded. This work provides new data for assessing the fate of radionuclides in the soil.

Author Contributions: Conceptualization, M.L. and Z.L.; validation, D.X. and M.L.; writing original draft paper, Y.S. and Y.Z.; editing; G.Z.; funding acquisition, L.M. All authors have read and agreed to the published. All authors have read and agreed to the published version of the manuscript.

Funding: This work was funded by the National Science Foundation of China (Grants 12275301; 12105311); Ministry Science and Technology of China (Grant Number: 2022xjkk0300), and the Innovation Fund of Institute of High Energy Physics, Chinese Academy of Sciences (20221117174337).

Data Availability Statement: Not applicable.

Conflicts of Interest: The authors declare no conflict of interest.

References

- Sasaki, T.; Matoba, D.; Dohi, T.; Fujiwara, K.; Kobayashi, T.; Iijima, K. Vertical distribution of ⁹⁰Sr and ¹³⁷Cs in soils near the Fukushima Daiichi nuclear power station. *J. Radioanal. Nucl. Chem.* **2020**, *326*, 303–314. [CrossRef]
- Shao, Y.; Yang, G.; Tazoe, H.; Ma, L.; Yamada, M.; Xu, D. A review of measurement methodologies and their applications to environmental ⁹⁰Sr. *J. Environ. Radioact.* **2018**, *192*, 323–333. [CrossRef]
- Dulanská, S.; Cocha, I.; Silliková, V.; Goneková, Z.; Horváthová, B.; Nodilo, M.; Grahek, Z. Sequential determination of ⁹⁰Sr and ²¹⁰Pb in bone samples using molecular recognition technology product AnaLig@Sr-01. *Microchem. J.* **2020**, *157*, 105123. [CrossRef]
- Deng, F.; Lin, F. Measurement of ⁹⁰Sr in Marine Biological Samples. *Molecules* **2022**, *27*, 3730. [CrossRef] [PubMed]
- Xu, P.; Ding, C.; Yu, G.; Chen, Z. Determination of ⁹⁰Sr in different matrices via ion-exchange chromatography and LSC. *J. Radioanal. Nucl. Chem.* **2022**, *331*, 3269–3274. [CrossRef]
- Zhong, N.; Li, L.; Yang, X.; Zhao, Y. Analytical Methods for the Determination of ⁹⁰Sr and ^{239,240}Pu in Environmental Samples. *Molecules* **2022**, *27*, 1912. [CrossRef]
- Mamikhin, S.; Lipatov, D.; Manakhov, D.; Paramonova, T.; Stolbova, V.; Shcheglov, A. Adaptive capability of the vert_mig algorithm to simulate vertical migration of radionuclides in soils. *Mosc. Univ. Soil Sci. Bull.* **2018**, *73*, 11–17. [CrossRef]
- Marchesani, G.; Trotta, G.; De Felice, P.; Marchesani, G.; Bortone, N.; Damiano, R.; Nicolini, M.; Accettulli, R.; Chiaravalle, A.E. Fast and Sensitive Radiochemical Method for Sr-90 Determination in Food and Feed by Chromatographic Extraction and Liquid Scintillation Counting. *Food Anal. Method* **2022**, *15*, 1521–1534. [CrossRef]

9. Wang, Z.; Zhang, Y.; Flury, M.; Zou, H. Freeze-thaw cycles lead to enhanced colloid-facilitated Pb transport in a Chernozem soil. *J. Contam. Hydrol.* **2022**, *251*, 104093. [[CrossRef](#)]
10. Zhao, Y.; Shao, Z.; Chen, C.; Hu, J.; Chen, H. Effect of environmental conditions on the adsorption behavior of Sr (II) by na-rectorite. *Appl. Clay Sci.* **2014**, *87*, 1–6. [[CrossRef](#)]
11. Albarran, N.; Missana, T.; García-Gutiérrez, M.; Alonso, U.; Mingarro, M. Strontium migration in a crystalline medium: Effects of the presence of bentonite colloids. *J. Contam. Hydrol.* **2011**, *122*, 76–85. [[CrossRef](#)]
12. Sun, Y.; Zhang, H.; Lee, C.; Luo, M.; Hua, R.; Liu, W.; Kong, J.; Hu, Y. Diffusion behavior of Se(IV) in Tamusu clayrock core by through-diffusion method. *J. Radioanal. Nucl. Chem.* **2021**, *329*, 149–158. [[CrossRef](#)]
13. Wang, C.; Myshkin, V.F.; Khan, V.A.; Panamareva, A.N. A review of the migration of radioactive elements in clay minerals in the context of nuclear waste storage. *J. Radioanal. Nucl. Chem.* **2022**, *331*, 3401–3426. [[CrossRef](#)]
14. Amayri, S.; Fröhlich, D.R.; Kaplan, U.; Trautmann, N.; Reich, T. Distribution coefficients for the sorption of Th, U, Np, Pu, and Am on Opalinus Clay. *Radiochim. Acta* **2016**, *104*, 33–40. [[CrossRef](#)]
15. Singh, B.; Tomar, R.; Kumar, S.; Kar, A.; Tomar, B.; Ramanathan, S.; Manchanda, V. Role of the humic acid for sorption of radionuclides by synthesized titania. *Radiochim. Acta* **2014**, *102*, 255–261. [[CrossRef](#)]
16. Wang, X.; Chen, C.; Du, J.; Tan, X.; Xu, D.; Yu, S. Effect of pH and aging time on the kinetic dissociation of ²⁴³Am (III) from humic acid-coated γ -Al₂O₃: A chelating resin exchange study. *Environ. Sci. Technol.* **2005**, *39*, 7084–7088. [[CrossRef](#)] [[PubMed](#)]
17. Mishra, S.; Maity, S.; Bhalke, S.; Pandit, G.; Puranik, V.; Kushwaha, H. Thermodynamic and kinetic investigations of uranium adsorption on soil. *J. Radioanal. Nucl. Chem.* **2012**, *294*, 97–102. [[CrossRef](#)]
18. Xia, L.; Huang, X.; Cao, C.C. Sorption and mechanism of aqueous U(VI) onto red soil-colloid. *Energy Sci. Tech.* **2013**, *47*, 1692–1699.
19. Jiang, W.; Li, Z.; Xie, H.; Ouyang, K.; Yuan, H.; Duan, L. Land use change impacts on red slate soil aggregates and associated organic carbon in diverse soil layers in subtropical China. *Sci. Total Environ.* **2023**, *856*, 159194. [[CrossRef](#)]
20. Leão, T.P.; Barros Guimarães, T.L.; de Figueiredo, C.C.; Galba Busato, J.; Sato Breyer, H. On critical coagulation concentration theory and grain size analysis of oxisols. *Soil Sci. Soc. Am. J.* **2013**, *77*, 1955–1964. [[CrossRef](#)]
21. Mikutta, R.; Kleber, M.; Kaiser, K.; Jahn, R. Organic matter removal from soils using hydrogen peroxide, sodium hypochlorite, and disodium peroxodisulfate. *Soil Sci. Soc. Am. J.* **2005**, *69*, 120–135. [[CrossRef](#)]
22. Romero, A.; Santos, A.; Cordero, T.; Rodríguez-Mirasol, J.; Rosas, J.M.; Vicente, F. Soil remediation by Fenton-like process: Phenol removal and soil organic matter modification. *Chem. Eng. J.* **2011**, *170*, 36–43. [[CrossRef](#)]
23. Huang, Z.; Li, Z.; Zheng, L.; Zhou, L.; Chai, Z.; Wang, X.; Shi, W. Interaction mechanism of uranium(VI) with three-dimensional graphene oxide-chitosan composite: Insights from batch experiments, IR, XPS, and EXAFS spectroscopy. *Chem. Eng. J.* **2017**, *328*, 1066–1074. [[CrossRef](#)]
24. Du, Y.; Yin, Z.; Wu, H.; Li, P.; Qi, W.; Wu, W. Sorption of U (VI) on magnetic illite: Effects of pH, ions, humic substances and temperature. *J. Radioanal. Nucl. Chem.* **2015**, *304*, 793–804. [[CrossRef](#)]
25. Guimaraes, V.; Azenha, M.; Rocha, F.; Silva, F.; Bobos, I. Batch and flow-through continuous stirred reactor experiments of Sr²⁺ adsorption onto smectite: Influence of pH, concentration and ionic strength. *J. Radioanal. Nucl. Chem.* **2012**, *303*, 2243–2255.
26. Ji, G.; Xu, M.; Wen, S.; Wang, B.; Zhang, L.; Liu, L. Characteristics of soil pH and exchangeable acidity in red soil profile under different vegetation types. *J. Appl. Eco.* **2015**, *26*, 2639–2645.
27. Hu, J.; Chen, C.; Sheng, G.; Li, J.; Chen, Y.; Wang, X. Adsorption of Sr (II) and Eu (III) on Na-rectorite: Effect of pH, ionic strength, concentration and modelling. *Radiochim. Acta* **2010**, *98*, 421–429. [[CrossRef](#)]
28. Hongxia, Z.; Xiaoyun, W.; Honghong, L.; Tianshe, T.; Wangsuo, W. Adsorption behavior of Th (IV) onto illite: Effect of contact time, pH value, ionic strength, humic acid and temperature. *Appl. Clay Sci.* **2016**, *127*, 35–43. [[CrossRef](#)]
29. Lu, Y.; Yu, J.; Cheng, S. Magnetic composite of Fe₃O₄ and activated carbon as a adsorbent for separation of trace Sr (II) from radioactive wastewater. *J. Radioanal. Nucl. Chem.* **2015**, *303*, 2371–2377. [[CrossRef](#)]
30. Chen, L.; Dong, Y. Sorption of ⁶³Ni (II) to montmorillonite as a function of pH, ionic strength, foreign ions and humic substances. *J. Radioanal. Nucl. Chem.* **2013**, *295*, 2117–2123. [[CrossRef](#)]
31. Yan, D.; Zuo, R.; Ding, K.; Wang, T.; Fan, L.; He, Y.; Jiang, X. Influencing factors of ⁹⁰Sr adsorption onto granite fracture filling material in a high-level radioactive waste disposal site. *J. Radioanal. Nucl. Chem.* **2022**, *331*, 2679–2688. [[CrossRef](#)]
32. Guedes, R.S.; Fernandes, A.R.; Souza, E.S.d.; Silva, J.R.R.e. Maximum phosphorus adsorption capacity adjusted to isotherm models in representative soils of eastern amazon. *Commun. Soil Sci. Plant Anal.* **2015**, *46*, 2615–2627. [[CrossRef](#)]
33. Basse, U.; Suleiman, M.; Ochigbo, S.; Ndamitso, M.; Daniel, E.; Otolu, S.; Chukwudi, A. Adsorption isotherm, kinetics and thermodynamics study of Cr (VI) ions onto modified activated carbon from endocarp of *Canarium schweinfurthii*. *Int. Res. J. Pure Appl. Chem.* **2015**, *6*, 46–55. [[CrossRef](#)]
34. Peng, X.; Yan, X.; Zhou, H.; Zhang, Y.; Sun, H. Assessing the contributions of sesquioxides and soil organic matter to aggregation in an ultisol under long-term fertilization. *Soil Tillage Res.* **2015**, *146*, 89–98. [[CrossRef](#)]
35. Sun, C.; Liu, J.; Wang, Y.; Zheng, N.; Wu, X.; Liu, Q. Effect of long-term cultivation on soil organic carbon fractions and metal distribution in humic and fulvic acid in black soil, Northeast China. *Soil Res.* **2012**, *50*, 562–569. [[CrossRef](#)]
36. Zhao, D.; Yang, S.; Chen, S.; Guo, Z.; Yang, X. Effect of pH, ionic strength and humic substances on the adsorption of Uranium (VI) onto Na-rectorite. *J. Radioanal. Nucl. Chem.* **2011**, *287*, 557–565. [[CrossRef](#)]
37. Tangestani, F.; Rashidi, A.; Mallah, M.-H. The kinetic study of cesium, strontium, and rubidium Radionuclide's adsorption from synthetic and natural wastes via the mag-molecular process. *Water Air Soil Pollut.* **2017**, *228*, 1–13. [[CrossRef](#)]

38. Deepthi Rani, R.; Sasidhar, P. Sorption of cesium on clay colloids: Kinetic and thermodynamic studies. *Aquat. Geochem.* **2012**, *18*, 281–296. [[CrossRef](#)]
39. Mosquera-Vivas, C.S.; Obregon-Neira, N.; Celis-Ossa, R.E.; Guerrero-Dallos, J.A.; González-Murillo, C.A. Degradation and thermodynamic adsorption process of carbofuran and oxadicyl in a colombian agricultural soil profile. *Agron. Colomb.* **2016**, *34*, 92–100. [[CrossRef](#)]
40. Li, C.; Wang, S.; Ji, F.; Zhang, J.; Wang, L. Thermodynamics of Cu^{2+} adsorption on soil humin. *Int. J. Environ. Res.* **2015**, *9*, 43–52.
41. He, Y.; Chen, Y.G.; Ye, W.M. Equilibrium, kinetic, and thermodynamic studies of adsorption of Sr(II) from aqueous solution onto GMZ bentonite. *Environ. Earth Sci.* **2016**, *75*, 807–817. [[CrossRef](#)]

Disclaimer/Publisher's Note: The statements, opinions and data contained in all publications are solely those of the individual author(s) and contributor(s) and not of MDPI and/or the editor(s). MDPI and/or the editor(s) disclaim responsibility for any injury to people or property resulting from any ideas, methods, instructions or products referred to in the content.